[13] I. D. Walker, "The control of kinematically redundant robot manipulators," M.S. thesis, The University of Texas at Austin, Austin, TX, 1985.

[14] T. Yoshikawa, "Analysis and control of robot manipulators with redundancy," in Robotics Research—The First International Symposium, Brady and Paul, Eds. Cambridge, MA: MIT Press, 1984, pp. 735–748.

[15] ——, "Manipulability and redundancy control of robotic mechanisms," in Proc. 1985 IEEE Int. Conf. on Robotics and Automation (St. Louis, MO, 1985).

# Kinematic Analysis of a Three-Degrees-of-Freedom In-Parallel Actuated Manipulator

KOK-MENG LEE AND DHARMAN K. SHAH

*Abstract*—This communication presents an alternative design of a three-degrees-of-freedom manipulator based on the concept on an in-parallel actuated mechanism. The manipulator has two degrees of orientation freedom and one degree of translatory freedom. The basic kinematic equations for use of the manipulator are derived and the influences of the physical constraints on the range of motion in the practical design are discussed. Several possible applications which include the in-parallel mechanism as part of the manipulation system are suggested.

## I. INTRODUCTION

Industrial robots have traditionally been used as general-purpose positioning devices and are anthropomorphic open-chain mechanisms which generally have the links actuated in series. The open kinematic chain manipulators usually have longer reach, larger workspace, and more dextrous maneuverability in reaching small space. However, the cantilever-like manipulator is inherently not very rigid and has poor dynamic performance at high-speed and high dynamic loading operating conditions. Due to several increasingly important classes of robot applications, especially automatic assembly, data-driven manufacturing and reconfigurable jigs and fixtures assembly for high-precision machining, significant effort has been directed towards finding techniques for improving the effective accuracy of the open-chain manipulator with calibration methods [1], compliance methods [2]–[5], and endpoint sensing methods [6], [7].

Recently, some effort has been directed towards the investigation of alternative manipulator designs based on the concepts of closed kinematic chain due to the following advantages as compared to the traditional open kinematic chain manipulators: more rigidity and accuracy due to the lack of cantilever-like structure, high force/torque capacity for the number of actuators as the actuators are

arranged in parallel rather than in series, and relatively simpler inverse kinematics which is an advantage in real-time computer on-line control. The closed kinematic chain manipulators have potential applications where the demand on workspace and maneuverability is low but the dynamic loading is severe and high speed and precision motion are of primary concerns. Typical examples of in-parallel mechanism are a camera tripod and a six-degrees-of-freedom Steward platform which has been originally designed as an aircraft simulator [8], [9] and later as a robot wrist [10]. Various applications of the Steward platform have been investigated for use in mechanized assembly [11] and for use as a compliance device [12]. Significant effort has been directed towards tendon actuated in-parallel manipulators [13], [14] which have the advantages of high force-to-weight ratio. A systematic review on possible alternative in-parallel mechanisms and other combinations in which part of the manipulator is serial and part parallel have been addressed in [15], [16]. The kinematics and practical design consideration have been discussed in [17], [18].

The manipulation approach analyzed in this communication is based on an in-parallel actuated tripod-like manipulator which has two degrees of orientation freedom and one degree of translatory freedom. The purpose of this investigation is to develop an analytical method and systematic design procedures to analyze the basic kinematics. The influence of the physical constraints on the practical design imposed by the limits of the ball joints and the links on the kinematics are discussed.

## II. KINEMATICS EQUATIONS FOR THE THREE-DEGREES-OF-FREEDOM IN-PARALLEL ACTUATED MANIPULATOR

A schematic of an in-parallel manipulator is shown in Fig. 1. The manipulator consists of an upper platform which houses the driving mechanism of the gripper, three extensible links, and a base platform. The upper platform is connected to the links by means of ball joints which are equally spaced at $120°$ and at a radius $r$ from the center of the upper platform. The other ends of the links are connected to the base platform through equally spaced pin joints at a radius $R$ from the center of the base platform. By varying the link lengths, the upper platform can be manipulated with respect to the base platform.

A base Cartesian coordinate frame $XYZ$ is fixed at the center of the base platform with the $Z$-axis pointing vertically upward and the $X$-axis pointing towards the pin joint 1, $P_1$. Similarly, a coordinate frame $xyz$ is assigned to the center of the upper platform, with the $z$-axis normal to the platform and the $x$-axis pointing towards the ball joint 1, $B_1$. Hence the coordinates of the pin joints in $XYZ$ frame are

$$P_1 = \begin{bmatrix} R \\ 0 \\ 0 \end{bmatrix}$$

$$P_2 = \begin{bmatrix} -\dfrac{1}{2}R \\ \dfrac{\sqrt{3}}{2}R \\ 0 \end{bmatrix}$$

$$P_3 = \begin{bmatrix} -\dfrac{1}{2}R \\ -\dfrac{\sqrt{3}}{2}R \\ 0 \end{bmatrix} \tag{1}$$
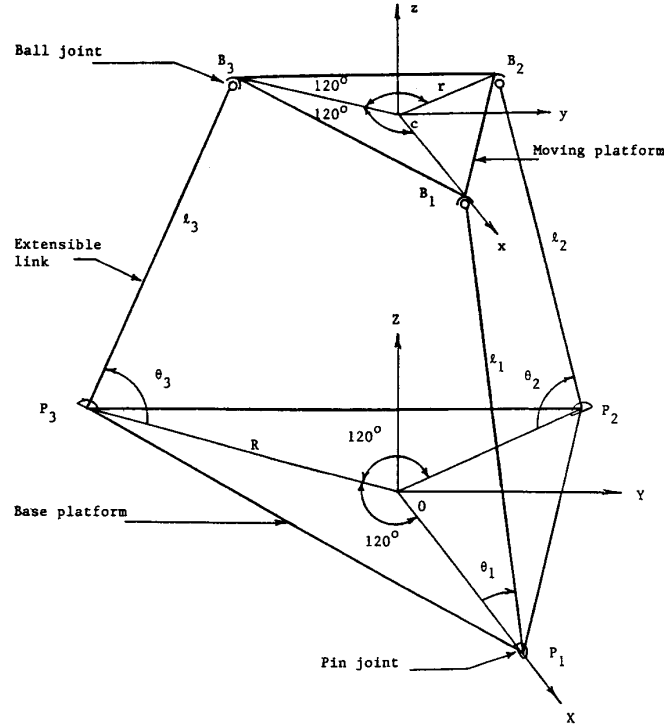
Fig. 1. Three-degrees-of-freedom in-parallel actuated mechanism schematic.

and coordinates of the ball joints in $xyz$ frame are

$$b_1 = \begin{bmatrix} r \\ 0 \\ 0 \end{bmatrix}$$

$$b_2 = \begin{bmatrix} -\dfrac{1}{2} r \\ \dfrac{\sqrt{3}}{2} r \\ 0 \end{bmatrix}$$

$$b_3 = \begin{bmatrix} -\dfrac{1}{2} r \\ -\dfrac{\sqrt{3}}{2} r \\ 0 \end{bmatrix}. \qquad (2)$$

The coordinate frame $xyz$ with respect to the base coordinate frame $XYZ$ can be described by the homogeneous transformation $[T]$

$$[T] = \begin{bmatrix} n_1 & o_1 & a_1 & X_c \\ n_2 & o_2 & a_2 & y_c \\ n_3 & o_3 & a_3 & z_c \\ 0 & 0 & 0 & 1 \end{bmatrix} \qquad (3)$$

where $(x_c, y_c, z_c)^T$ describes the position of the origin of the $xyz$ frame and the orientation vectors $(n_1, n_2, n_3)^T$, $(o_1, o_2, o_3)^T$, and $(a_1, a_2, a_3)^T$ are the directional cosines of the axes $x$, $y$, and $z$ with respect to the base frame $XYZ$. As the unit vectors $n$, $o$, and $a$ form a orthonormal set, there are six constraint equations on the nine

elements, i.e.,

$$n \cdot n = 1$$

$$o \cdot o = 1$$

$$a \cdot a = 1$$

$$o \cdot a = 0$$

$$o \cdot n = 0$$

$$a \cdot n = 0. \qquad (4)$$

The Cartesian position of the ball joints with respect to the base frame $XYZ$ can be expressed as

$$\begin{bmatrix} B_i \\ 1 \end{bmatrix}_{XYZ} = [T] \begin{bmatrix} b_i \\ 1 \end{bmatrix}_{xyz} \qquad (5)$$

where the vectors $B_i$ and $b_i$ describe the position vectors of the $i$th ball joint with respect to the base frame $XYZ$ and frame $xyz$, respectively. The length of the link, which is equal to the distance between the $i$th ball joint and the $i$th pin joint is

$$L_1^2 = (n_1\rho + X_c - 1)^2 + (n_2\rho + Y_c)^2 + (n_3\rho + Z_c)^2 \qquad (6)$$

$$L_2^2 = \frac{1}{4} [(-n_1\rho + \sqrt{3}o_1\rho + 2X_c + 1)^2$$

$$+ (-n_2\rho + \sqrt{3}o_2\rho + 2Y_c - \sqrt{3})^2$$

$$+ (-n_3\rho + \sqrt{3}o_3\rho + 2Z_c)^2] \qquad (7)$$

$$L_3^2 = \frac{1}{4} [(-n_1\rho - \sqrt{3}o_1\rho + 2X_c + 1)^2$$

$$+ (-n_2\rho - \sqrt{3}o_2\rho + 2Y_c + \sqrt{3})^2$$

$$+ (-n_3\rho - \sqrt{3}o_3\rho + 2Z_c)^2] \qquad (8)$$

where

$$\rho = \frac{r}{R}$$

$$L_i = \frac{l_i}{R}, \qquad i = 1, 2, 3$$

and

$$X_c = \frac{x_c}{R} \qquad Y_c = \frac{y_c}{R} \qquad Z_c = \frac{z_c}{R}.$$

As the links $P_1B_1$, $P_2B_2$, and $P_3B_3$ are constrained by the pin joints to move in the planes, $y = 0$, $y = -\sqrt{3}\,x$, and $y = +\sqrt{3}\,x$, respectively, the constraint equations imposed by the pin joints are

$$n_2\rho + Y_c = 0 \tag{9}$$

$$-n_2\rho + \sqrt{3}\,o_2\rho + 2Y_c = -\sqrt{3}[-n_1\rho + \sqrt{3}\,o_1\rho + 2X_c] \tag{10}$$

$$-n_2\rho - \sqrt{3}\,o_2\rho + 2Y_c = \sqrt{3}[-n_1\rho - \sqrt{3}\,o_1\rho + 2X_c]. \tag{11}$$

By adding (10) and (11) and subtracting (10) from (11), respectively, the constraints (10) and (11) can be simplified as

$$n_2 = o_1 \tag{12}$$

$$X_c = \frac{\rho}{2}(n_1 - o_2). \tag{13}$$

As (12) imposes an orientation constraint in addition to that described in (4), only two of the nine directional cosines are independent. Equations (9) and (13) relate $X_c$ and $Y_c$ to the directional cosines. Hence, the manipulator has only two degrees of freedom in orientation and one degree of freedom in Cartesian position.

Equations (6)–(8) are the inverse kinematic equations which define the actuating length of the links for a prescribed position and orientation of the moving platform. To compute the link lengths using (6)–(8), both the position and orientation of the moving frame, i.e., six variables, must be defined. As the system has three degrees of freedom, only three of the six position/orientation variables are independent and the remaining dependent variables must be calculated from (5), (9), (12), and (13).

A more compact form of solutions for the link lengths can be obtained by expressing the directional cosines in terms of $Z$-$Y$-$Z$ Euler angles $(\alpha, \beta, \gamma)$ [19] as

$$\alpha = \text{Atan } 2(a_2, a_1) \tag{14}$$

$$\beta = \text{Atan } 2(\sqrt{n_3^2 + o_3^2}, a_3) \tag{15}$$

$$\gamma = \text{Atan } 2(o_3, -n_1) \tag{16}$$

where $0 < \beta < \pi$. Equation (12) becomes

$$\alpha + \gamma = n\pi, \qquad n = 0, \pm 1, \pm 2. \tag{17}$$

Mathematically, two possible sets of link lengths for a specified set of $\alpha$, $\beta$ and $Z_c$, can be obtained depending on whether $n$ is even or odd. As there are physical constraints imposed by the limits of the ball joints, only $n$ equal to zero is physically realizable.

$$X_c = -\frac{1}{2}\rho(1 - C_\beta)C_{2\alpha} \tag{18}$$

$$Y_c = \frac{1}{2}\rho(1 - C_\beta)S_{2\alpha} \tag{19}$$

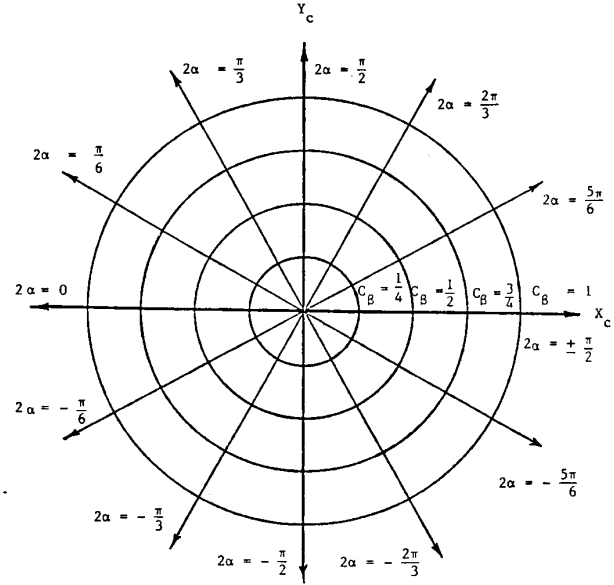where $C_\beta = \cos \beta$, $S_{2\alpha} = \sin 2\alpha$, and $C_{2\alpha} = \cos 2\alpha$.



Fig. 2. Plots showing relation between Euler angles $\alpha$, $\beta$ and Cartesian coordinates $X_c$, $Y_c$.

The Cartesian position, $X_c$ and $Y_c$, can be expressed graphically as a function of $\alpha$ and $\beta$ as shown in Fig. 2. The constant $\cos \beta$ plots are essentially a family of concentric circles with the radii linearly proportional to trigonometric cosines of $\beta$ and the constant $\alpha$ plots are a family of straight radial lines originating from the origin with the slopes equal to $\tan(-2\alpha)$. The algebraic sign of $X_c$ and $Y_c$ depends on the value of $2\alpha$ as shown in Fig. 2.

The link lengths in terms of Euler angles are

$$\begin{aligned} L_1^2 &= 1 + \rho^2 + X_c^2 + Y_c^2 + Z_c^2 - 2X_c \\ &\quad + 2\rho(C_\alpha^2 C_\beta + S_\alpha^2)(X_c - 1) \\ &\quad + \rho(C_\beta - 1)S_{2\alpha}Y_c \\ &\quad - 2\rho S_\beta C_\alpha Z_c \end{aligned} \tag{20}$$

$$\begin{aligned} L_2^2 &= 1 + \rho^2 + X_c^2 + Y_c^2 + Z_c^2 + X_c - \sqrt{3}\,Y_c \\ &\quad - \rho[C_\alpha^2 C_\beta + S_\alpha^2 - \sqrt{3}\,C_\alpha S_\alpha(C_\beta - 1)]\left[X_c + \frac{1}{2}\right] \\ &\quad - \rho[S_\alpha C_\alpha(C_\beta - 1) - \sqrt{3}(S_\alpha^2 C_\beta + C_\alpha^2)]\left[Y_c - \frac{\sqrt{3}}{2}\right] \\ &\quad + \rho S_\beta[C_\alpha - \sqrt{3}\,S_\alpha]Z_c \end{aligned} \tag{21}$$

$$\begin{aligned} L_3^2 &= 1 + \rho^2 + X_c^2 + Y_c^2 + Z_c^2 + X_c + \sqrt{3}\,Y_c \\ &\quad - \rho[C_\alpha^2 C_\beta + S_\alpha^2 - \sqrt{3}\,C_\alpha S_\alpha(C_\beta - 1)]\left[X_c + \frac{1}{2}\right] \\ &\quad - \rho[S_\alpha C_\alpha(C_\beta - 1) + \sqrt{3}(S_\alpha^2 C_\beta + C_\alpha^2)]\left[Y_c + \frac{\sqrt{3}}{2}\right] \\ &\quad + \rho S_\beta[C_\alpha + \sqrt{3}\,S_\alpha]Z_c \end{aligned} \tag{22}$$

where $S_\alpha = \sin \alpha$, $C_\alpha = \cos \alpha$, and $S_\beta = \sin \beta$. Hence, the independent variables are $\alpha$, $\beta$, and $Z_c$ and the dependent variables $\gamma$, $X_c$, and $Y_c$ are defined in (17)–(19), respectively.

## III. FORWARD KINEMATICS

The inverse kinematic discussed in the previous section must generally be computed on-line for real-time trajectory control of the manipulator. In dynamic analysis of the manipulator, both the forward kinematic which transforms the given actuator coordinates to Cartesian coordinates and the inverse kinematic are necessary. The forward kinematic involves solving the six simultaneous equations for the position/orientation in terms of the given line lengths. An alternative method to solve for the forward kinematics can be derived by noting the fact that the in-parallel actuated manipulator is essentially a structure for given link lengths.

The angles $\theta_1$, $\theta_2$, and $\theta_3$ are defined to be the angles between the links $L_1$, $L_2$, and $L_3$ and the base platform, respectively. As the distance between any two adjacent ball joints is $\sqrt{3}\ r$, $\theta_i$ can be related to $L_i$ implicitly using (5) as

$$L_1^2 + L_2^2 + 3 - 3\rho^2 + L_1 L_2 \cos\theta_1 \cos\theta_2 - 2L_1 L_2 \sin\theta_1 \sin\theta_2$$
$$- 3L_1 \cos\theta_1 - 3L_2 \cos\theta_2 = 0 \quad (23)$$

$$L_2^2 + L_3^2 + 3 - 3\rho^2 + L_2 L_3 \cos\theta_2 \cos\theta_3 - 2L_2 L_3 \sin\theta_2 \sin\theta_3$$
$$- 3L_2 \cos\theta_2 - 3L_3 \cos\theta_3 = 0 \quad (24)$$

$$L_3^2 + L_1^2 + 3 - 3\rho^2 + L_3 L_1 \cos\theta_3 \cos\theta_1 - 2L_3 L_1 \sin\theta_3 \sin\theta_1$$
$$- 3L_3 \cos\theta_3 - 3L_1 \cos\theta_1 = 0 \quad (25)$$

where the coordinates of the ball joints with respect to the base frame are

$$X_{b1} = 1 - L_1 \cos\theta_1$$

$$Y_{b1} = 0$$

$$Z_{b1} = L_1 \sin\theta_1 \quad (26)$$

$$X_{b2} = -\frac{1}{2}(1 - L_2 \cos\theta_2)$$

$$Y_{b2} = +\frac{\sqrt{3}}{2}(1 - L_2 \cos\theta_2)$$

$$Z_{b2} = L_2 \sin\theta_2 \quad (27)$$

$$X_{b3} = -\frac{1}{2}(1 - L_3 \cos\theta_3)$$

$$Y_{b3} = -\frac{\sqrt{3}}{2}(1 - L_3 \cos\theta_3)$$

$$Z_{b3} = L_3 \sin\theta_3. \quad (28)$$

As the ball joints are placed at the vertices of an equilateral triangle, the Cartesian position or the origin of the moving frame, which is essentially the centroid of the triangle, can be determined as

$$X_c = \frac{1}{3}\sum_{i=1}^{3}\frac{x_{bi}}{R}$$

$$Y_c = \frac{1}{3}\sum_{i=1}^{3}\frac{y_{bi}}{R}$$

$$Z_c = \frac{1}{3}\sum_{i=1}^{3}\frac{z_{bi}}{R}. \quad (29)$$

The orientation can be calculated using (17)-(19).

## IV. PHYSICAL CONSTRAINTS

The equations derived above are for the general position/orientation of the moving platform. However, in the design of a practical
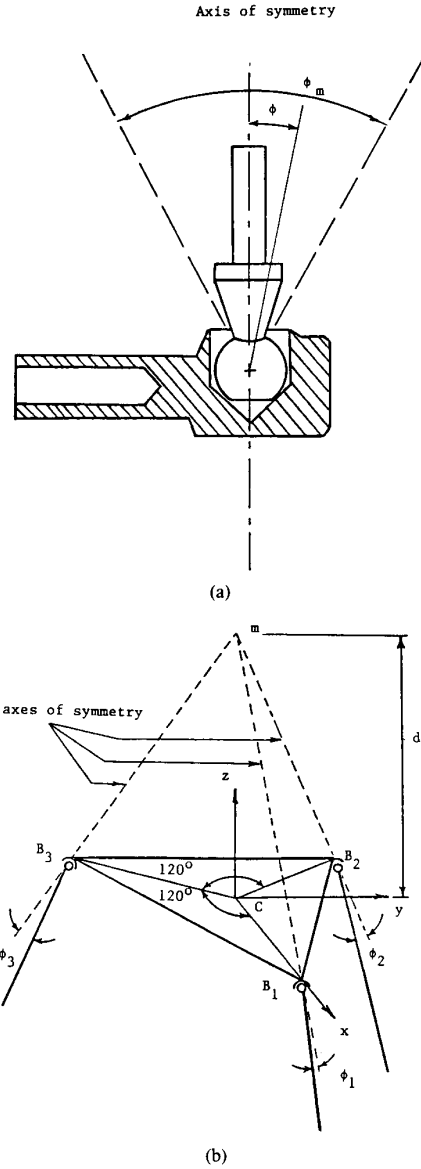


(a)



(b)

Fig. 3. (a) Ball-joint schematic. (b) Location of ball joints with respect to moving platform.

manipulator, there are physical constraints such as the limits of the ball joints and the actuating link lengths. Unlike the constraints imposed by the pin joints which limit the effective degrees of freedom, the physical constrains discussed in this section primarily limit the range of motion.

Fig. 3 shows a typical cross section of ball and socket joints where $\phi_i$ is the angle between the axis of symmetry of the ball joint and the link. The maximum angle of ball joints, $\phi_{max}$, has significant influence on the orientation of moving platform. The following derivation aims to express the angle $\phi_i$ as a function of the Cartesian position/orientation of the moving platform. If the normal vector $N$ of a plane containing the ball joints is

$$N = a_1 I + b_1 J + c_1 K \quad (30)$$

and the equation of the corresponding plane is
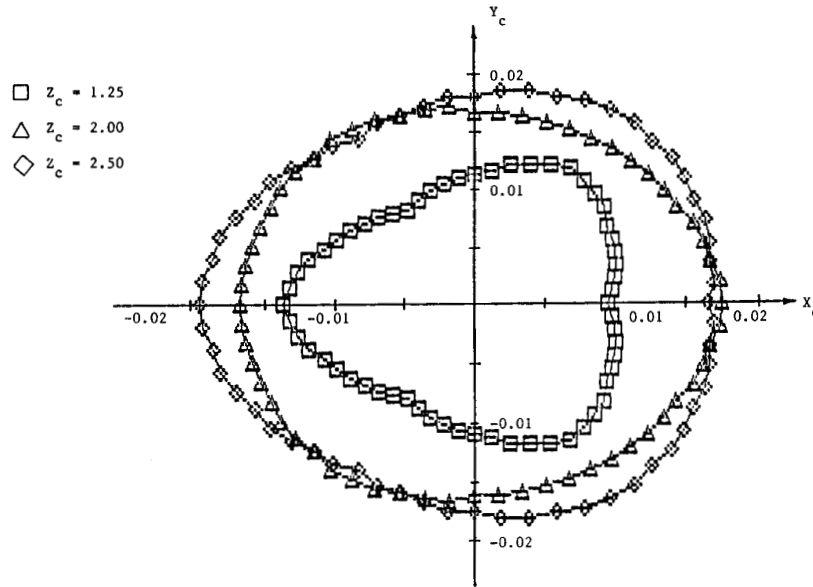
$$Ax + By + Cz = d \quad (31)$$

Fig. 4.   $X$-$Y$ plots of the work envelope of the in-parallel actuated mechanism.

we have

$$N = \overline{B_1 B_2} \times \overline{B_2 B_3} \tag{32}$$

where $B_1 B_2$ and $B_2 B_3$ are the line vectors directed from ball joints $B1$ to $B2$ and $B2$ to $B3$, respectively. With the Cartesian coordinates of the ball joints given in (5), the components of the normal vector $N$ can then be determined as

$$a_1 = \frac{3\sqrt{3}}{2} r^2 (n_2 o_3 - o_2 n_3)$$

$$b_1 = \frac{3\sqrt{3}}{2} r^2 (-n_1 o_3 + o_1 n_3)$$

$$c_1 = \frac{3\sqrt{3}}{2} r^2 (n_1 o_2 - o_1 n_2). \tag{33}$$

As the sockets of the ball joints are rigidly attached to the moving platform, the axis of symmetry of each socket intersects the normal of the plane at $m$. The equation of the line along the normal and passing through the point $(x_c, y_c, \text{and } z_c)$ is

$$\frac{x - x_c}{a_1} = \frac{y - y_c}{b_1} = \frac{z - z_c}{c_1}. \tag{34}$$

By defining the unit vector components such that

$$A = \frac{a_1}{\sqrt{a_1^2 + b_1^2 + c_1^2}}$$

$$B = \frac{b_1}{\sqrt{a_1^2 + b_1^2 + c_1^2}}$$

$$C = \frac{c_1}{\sqrt{a_1^2 + b_1^2 + c_1^2}} \tag{35}$$

(34) can be rewritten as

$$\frac{x_m - x_c}{A} = \frac{y_m - y_c}{B} = \frac{z_m - z_c}{C} = D_m. \tag{36}$$

Hence, the Cartesian coordinates of $m$ can be obtained as

$$x_m = x_c + A D_m$$

$$y_m = y_c + B D_m$$

$$z_m = z_c + C D_m. \tag{37}$$

Similarly, the equation of the line passing through the $i$th ball joint and the $i$th pin joint is

$$\frac{x - x_{pi}}{x_{bi} - x_{pi}} = \frac{y - y_{pi}}{y_{bi} - y_{pi}} = \frac{z - z_{pi}}{z_{bi} - z_{pi}}, \qquad i = 1, 2, 3. \tag{38}$$

Hence, the angle between the lines described by (34) and (38) is

$$\cos \phi_i = \frac{1}{\sqrt{(x_{bi} - x_{pi}) + (y_{bi} - y_{pi}) + (z_{bi} - z_{pi})}} \cdot \frac{(x_m - x_{bi})(x_{bi} - x_{pi}) + (y_m - y_{bi})(y_{bi} - y_{pi}) + (z_m - z_{bi})(z_{bi} - z_{pi})}{\sqrt{(x_m - x_{bi})^2 + (y_m - y_{bi})^2 + (z_m - z_{bi})^2}} \tag{39}$$

where $i = 1, 2, 3$, and $0 < \phi_i < \phi_{max}/2$.

A simulation of the kinematics of the three-degrees-of-freedom in-parallel actuated manipulator has been written to investigate the range of motion limited by the ball joints and the links. The simulation is done for an $X$-$Y$ plane with $Z_c$ held constant. The simulation shows the extremes of the $X_c$ and $Y_c$ for a given design. An example of the simulation output is shown in Fig. 4 for the following configuration:
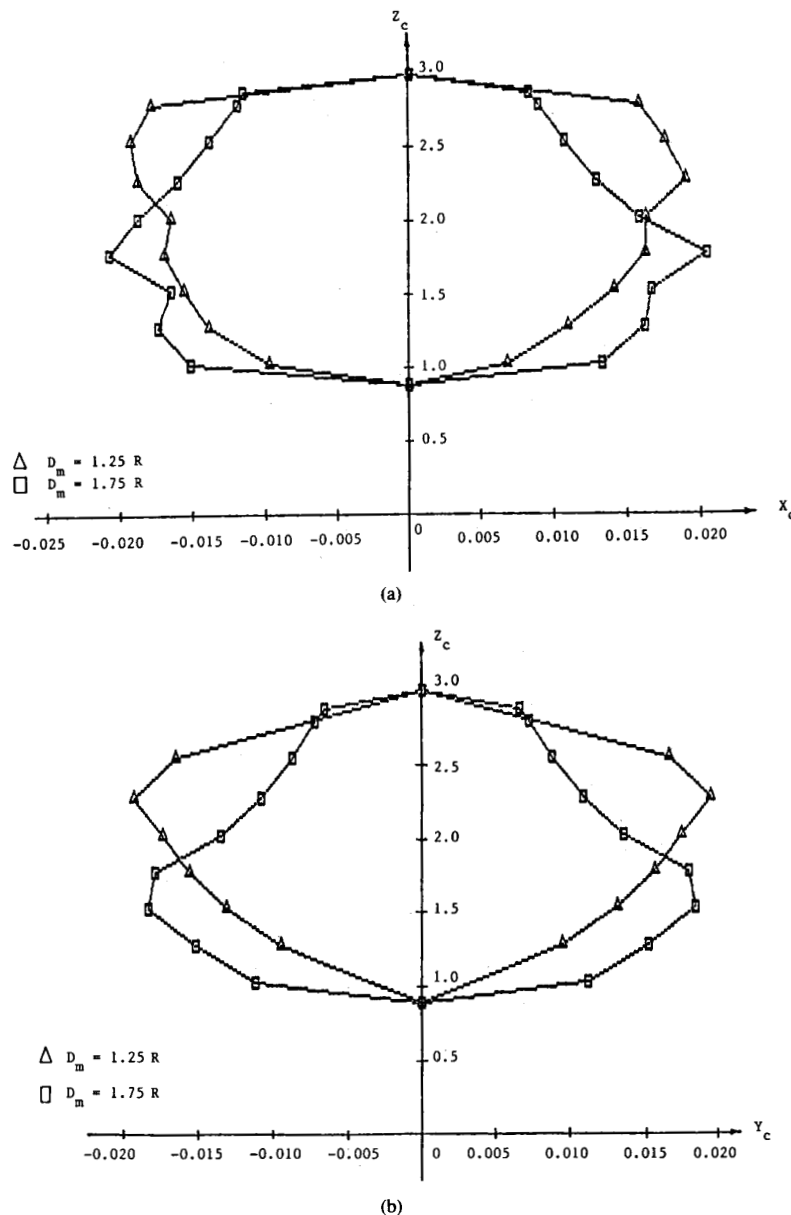
Fig. 5. (a) $X$–$Z$ plots of the work envelope of the in-parallel actuated mechanism. (b) $Y$–$Z$ plots of the work envelope of the in-parallel actuated mechanism.

the minimum and maximum link lengths are $R$ and $3R$, respectively, $\phi_{max}$ is 45°, and $D_m = 1.75$.

It is noted that the range of motion is primarily limited by the maximum angle of the ball joints except in the proximity of the minimum and maximum $Z_c$. Fig. 5 shows that the value of $D_m$ has a significant influence on the size and shape of the work envelope. The simulation output is useful in determining the range of motion and understanding the size and shape of work envelope. It also serves as a means of sizing the practical design parameters.

## V. APPLICATIONS

The in-parallel manipulator has potential applications where the orientation and reach in the $Z$ direction are more important than the translation in the $X$ and $Y$ directions. Apart from the suggestion made in [20] that a six-degrees-of-freedom arm could comprise two three-

degrees-of-freedom in-parallel actuated arms connected in series with one another, other possible applications of the manipulator as part of the six-degrees-of-freedom manipulation systems are shown in Fig. 6. In the manipulation system shown in Fig. 6(a) and (b), an additional rotational freedom is provided by the spin actuator and the translations in $X$ and $Y$ directions are obtainable by means of an $X$-$Y$ table. Typical applications are automated assembly, contour machining, and material handling. Fig. 6(c) shows a manipulator which combines an in-parallel actuated mechanism and a spherical wrist motor [21] to form a six-degrees-of-freedom dexterous end effector.

## VI. CONCLUSION

This communication presents the kinematic equations for use of a three-degrees-of-freedom in-parallel actuated mechanism as a robot
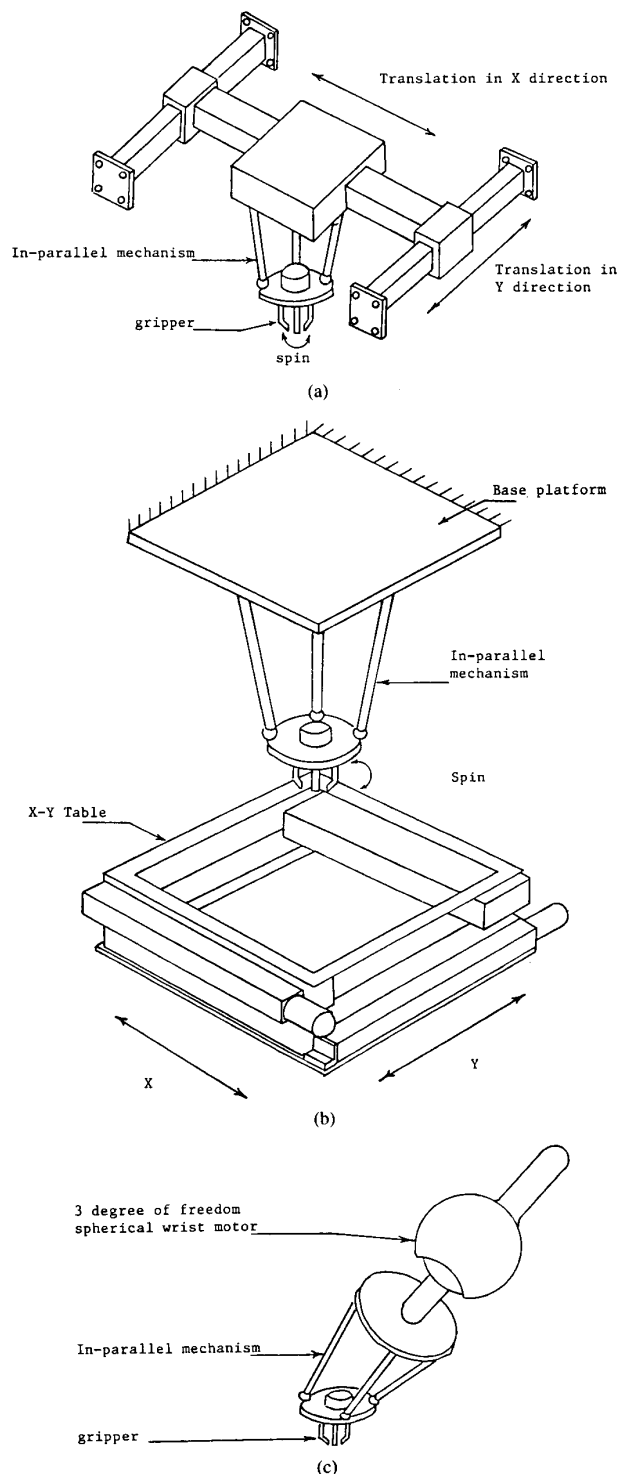
Fig. 6. (a) Schematic of an in-parallel actuated mechanism with moving Cartesian based frame. (b) Schematic of a six-degrees-of-freedom manipulator system which consists of an in-parallel actuated mechanism and an X-Y table. (c) Schematic of a six-degrees-of-freedom end effector based on a combination of in-parallel actuated mechanism and spherical wrist motor.

manipulator. The physical constraints imposed by the limits of the ball joints and the link lengths have been discussed. A simulation program has been developed to predict the range of motion for the purpose of practical design. Various possible applications of the in-parallel mechanism as part of the six-degrees-of-freedom manipulator are addressed. Future work should include dynamic analysis, prototype design, and evaluation in an industrial environment and computer-control scheme development.

REFERENCES

[1] R. Podoloff, W. Searing, and B. Hunter, "An accuracy test procedure for robotic manipulators utilizing a vision based, 3-D position sensing system," in *Proc. American Control Conf.* (San Diego, CA, June 1984).
[2] S. Drake, "Using compliance in lieu of sensory feedback for automatic assembly," D.Sc. dissertation MIT, Cambridge, MA, 1977.
[3] M. T. Mason, "Compliance and force control for computer controlled manipulators," *IEEE Trans. Syst., Man., Cybern.*, vol. SMC-11 no. 6, pp. 418-432, 1981.
[4] T. Lozaro-Perez, M. T. Mason, and R. H. Taylor, "Automatic synthesis of fine-motion strategies for manipulators," *Int. J. Robotics Res.*, vol. 3, no. 1, 1984.
[5] K. Asakawa, F. Akiya, and F. Tabata, "A variable compliance device and its application for automatic assembly," in *Proc. Autoface 5 Conf.* (Detroit, MI, Nov. 14-17, 1983).
[6] G. Beri, S. Hackwood, and W. S. Trimmer, "High-precision robot system for inspection and testing and electronic devices," in *Proc. IEEE Int. Conf. on Robotics* (Atlanta, GA, Mar. 1984).
[7] R. H. Taylor, R. L. Hollis, and M. A. Lavin, "Precise manipulation with endpoint sensing," *IBM J. Res. Devel.*, vol. 29, no. 4, July 1985.
[8] D. Stewart, "A platform with six degrees of freedom," *Proc. Inst. Mech. Eng.*, vol. 180, pt. 1, no. 15, pp. 371-386, 1965/1966.
[9] R. Hoffman and M. C. Hoffman, "Vibration modes of an aircraft simulation motion systems," in *Proc. 5th World Congr. for the Theory of Machines and Mechanisms* (an ASME, publ.), pp. 603-606, 1979.
[10] Bennett, "A mechanical wrist for a robot arm," B. S. thesis, MIT, Cambridge, MA, 1968.
[11] H. McCallion and P. D. Truong, "The analysis of a six-degree-of-freedom work station for mechanized assembly," in *Proc. 5th World Congr. for the Theory of Machines and Mechanisms* (an ASME publ.), pp. 611-616, 1979.
[12] H. McCallion, G. R. Johnson, and D. T. Phan, "A compliant device for inserting a peg into a hole," *The Industrial Robot*, June 1979.
[13] K. H. Lim, "Control of a tendon arm," MIT, Cambridge, MA, MIT A.I. Memo 617, Feb. 1981.
[14] S. E. Landsberger, "Design and construction of a cable-controlled, parallel link manipulator," MIT, Cambridge, MA, S. M. thesis, Sept. 1984.
[15] K. H. Hunt, "Structural kinematics of in-parallel-actuated robot arms," *Trans. ASME, J. Mech., Transmiss., Automat. Des.*, vol. 105, pp. 705-712, 1983.
[16] E. F. Fichter and E. D. McDowell, "A novel design for a robot arm," in *Advances in Computer Technology* (an ASME publ.), 1980, pp. 250-256.
[17] D. C. H. Yang and T. W. Lee, "Feasibility study of a platform type of robotic manipulators from a kinematic viewpoint," *J. Mech. Transmiss., Automat. Des.*, vol. 106, pp. 191-198, June 1984.
[18] E. F. Fichter, "A Steward platform-based manipulator: General theory and practical construction," *Int. J. Robotics Res.*, vol. 5, no. 2, Summer 1986.
[19] J. J. Craig, *Introduction to Robotics, Mechanics and Control*. Reading, MA: Addison-Wesley, 1985.
[20] K. H. Hunt, *Kinematic Geometry of Mechanisms*. London, UK: Oxford Univ. Press, 1978.
[21] K. Davey, G. Vachtesevanos, and R. Powers, "The analysis of fields and torques in a spherical induction motor," *IEEE Trans. Magn.*, vol. MAG-23, no. 1, pp. 273-282, Jan. 1987.